Compact MIMO Antenna for MUSIC-Based Angle of Arrival Estimation in Wrist-Worn Devices

Abel Zandamela
CONNECT Centre,
Trinity College Dublin
Dublin, Ireland
zandamea@tcd.ie

Nicola Marchetti
CONNECT Centre,
Trinity College Dublin
Dublin, Ireland
nicola.marchetti@tcd.ie

Adam Narbudowicz
CONNECT Centre,
Trinity College Dublin
Dublin, Ireland
narbudoa@tcd.ie

***Abstract*—In this work we propose a compact Multiple-Input Multiple-Output (MIMO) antenna for wrist-worn devices. The design is capable of unidirectional beamsteering across the entire horizontal plane, a property that is exploited for Angle of Arrival (AoA) Estimation based localization applications. The performance of the proposed system is evaluated using the high-resolution MUltiple SIgnal Classification (MUSIC) algorithm. Full-wave simulated results of the antenna in free-space show a peak realized gain of 5 dBi and estimated mean absolute errors $< 0.36°$. The gain and the estimated errors change to respectively 4.26 dBi and 0.45°, when using a human forearm phantom. The achieved results demonstrate the feasibility of the proposed antenna for localization applications using compact wrist-worn devices.**

Keywords–Angle of Arrival (AoA) Estimation, MUSIC algorithm, MIMO antennas, Wrist-worn devices, Localization techniques.

I. Introduction

Wrist-worn devices are becoming increasingly popular as new sensors are developed to enable increased functionalities such as smart health monitoring, security and localization [1]. However, wrist-wearable devices often suffer from reduced antenna efficiency, as they operate close to the human body. This results in a challenging design process for wrist-worn antennas, because they need to be compact and also account for body movements and coupling into the body [2]–[9].

In recent years, different antenna designs have been proposed to overcome the challenges posed by wrist-wearable devices [2]–[9]. An approach of integrating monopole and dipole antennas into the smartwatch belt is investigated in [3]. In [4], a technique that integrates a loop antenna into the front metal frame of a smartwatch device is proposed for Bluetooth applications. In the study presented in [5], two separate antennas (monopole and inverted-F antennas) are discussed for Global Positioning System (GPS) and Industrial, Scientific, and Medical (ISM band) wrist-worn devices. In [6] a variant of the planar inverted-F antenna is proposed for wrist-worn devices. In [7] a cavity-backed annular slot antenna is investigated for swartwatches with a metallic housing. The work in [8], exploits the theory of characteristic mode to design a multiple antenna system for wrist-worn devices. Lastly, a multi-band antenna is proposed for Long Term Evolution (LTE), Wideband Code Division Multiple Access (WCDMA), and ISM operations in wrist-wearable devices in [9].

The above discussed techniques present many advantages such as improved efficiency performance, compact and flexible integration into the wrist-worn devices, improved bandwidth and multi-band operations. However, these approaches are not capable of generating beam pattern reconfiguration, a property required for many indoor positioning systems, e.g.

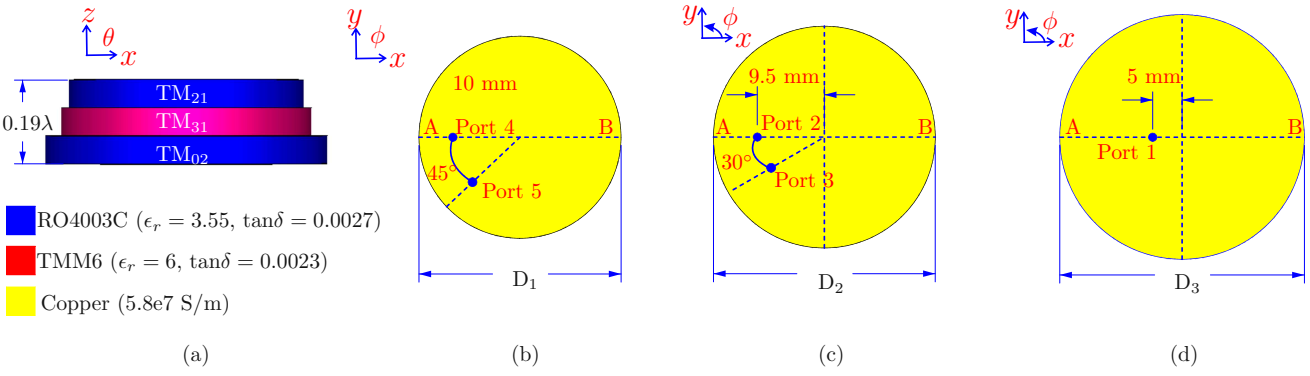

Fig. 1. Proposed system: (a) $xz-$plane of the proposed antenna with corresponding radiating modes; (b) Top-view with antenna diameter and marked ports for the top patch; (c) Diameter and marked ports for the middle patch and (d) diameter and port configuration of the bottom patch.

Angle of Arrival (AoA) estimation based localization systems; In fact these techniques often require larger antenna array structures (which are not suitable for wrist-worn devices) to generate the phase variations needed for AoA measurements. In this work, we propose for the first time in the open-literature, a compact MIMO antenna for Angle of Arrival (AoA) based localization from wrist-worn devices. The design has a diameter of 0.65λ (where λ is the wavelength at the antenna center operating frequency). Because the antenna is capable of unidirectional beamsteering over the entire azimuth plane, the AoA estimation performance is also investigated over the entire azimuth plane in free-space and including the effects of a human forearm phantom. The proposed system shows a peak realized gain of $4.26\,\text{dBi}$ and the estimated errors using the largest diameter of the analyzed phantom is below $0.45°$.

II. System Design

The proposed wrist-worn antenna is shown in Fig. 1. It includes three collocated patch structures and it is designed to operate at $5\,\text{GHz}$. The total thickness of the antenna is $11.6\,\text{mm}$ (0.19λ) [see Fig. 1(a)] and the diameter is D3 $= 39\,\text{mm}$ (0.65λ) [see Fig. 1(c)]. The bottom and top patches are made with RO4003C substrate [shown in blue in Fig. 1(a)], with relative permittivity $\epsilon_r = 3.55$ and tan $\delta = 0.0027$. For antenna miniaturization [10], the middle patch (diameter D2 $= 34.6\,\text{mm}$) is made on a substrate with a higher relative permittivity ($\epsilon_r = 6$ and tan $\delta = 0.0023$). Each patch on the proposed antenna is supported by a substrate with a height of $3.81\,\text{mm}$ and the patch is made of copper (thickness $= 0.035\,\text{mm}$).

The top and middle patch respectively excite two orthogonal TM_{21} and TM_{31} modes. This is done by feeding the top patch with port 4 at $10\,\text{mm}$ from the center towards **A** and port 5 oriented $45°$ in respect to port 4 [Fig. 1(b)] (see [11] for more details). The middle patch is also fed using two ports, with port 2 located at $9.5\,\text{mm}$ from the center towards **A** and port 3 oriented by $30°$ in respect to port 2 [as shown in Fig. 1(c)]. The bottom patch is fed using port 1 located at $5\,\text{mm}$ towards **A** [see Fig. 1(d)] and excites the TM_{02} mode. Because the bottom patch (exciting the TM_{02} mode) is the most efficient radiator within the excited modes, it is placed at the bottom. This technique allow its efficiency deterioration to stay within acceptable levels when the antenna is placed in direct contact with the human forearm phantom.

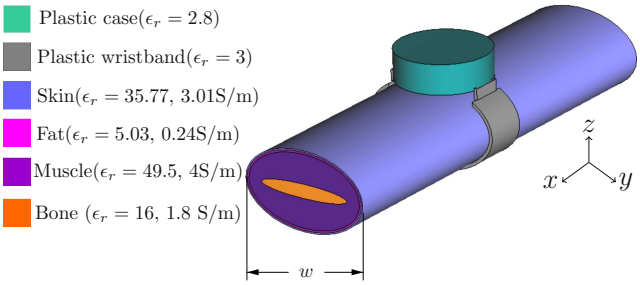

Fig. 2. Final set-up including plastic case, plastic wristband and human forearm-phantom (the antenna is placed inside the plastic case).

Fig. 2 shows the complete set-up used to investigate the performance of the antenna on the user's wrist. The system includes a forearm phantom (length $= 200\,\text{mm}$), plastic wristband (width $= 20\,\text{mm}$ and thickness $= 3\,\text{mm}$) and plastic case (diameter $= 43\,\text{mm}$ and $1\,\text{mm}$ of wall thickness). The antenna is placed at the phantom's center in direct contact with the skin layer and inside the plastic case. A gap of $1\,\text{mm}$ is introduced between the antenna and the plastic case.

The dielectric properties of the user's wrist tissues at $5\,\text{GHz}$ are reported in [12] and shown in Fig. 2. The phantom thickness is $36\,\text{mm}$ and the width is $w = 60\,\text{mm}$. The proportions of each phantom's layer are computed according to [13]. The skin and fat layers occupy 15% of the volume, the muscle layer 72.1% and the bone layer 12.9%.

III. Antenna Full-Wave Simulation

The proposed wrist-worn antenna is simulated using the

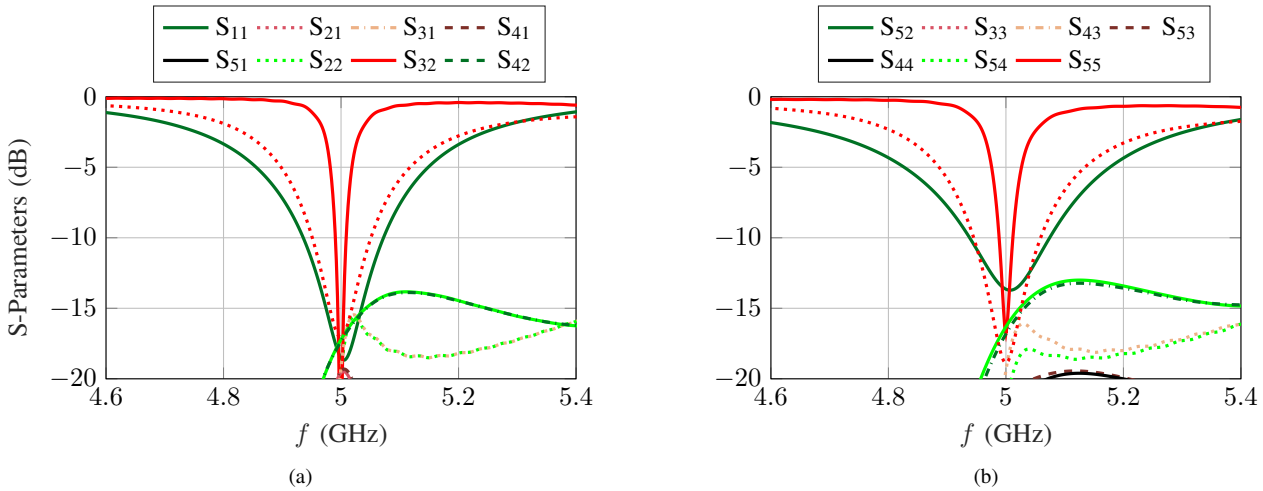

(a) (b)

Fig. 3. Full-wave simulated results: (a) S-parameters of the proposed antenna in free-space; (b) S-parameters of the antenna including the human forearm-phantom.

time-domain solver of the CST Studio Suite. The simulated S-parameters in free-space and with the forearm phantom are shown in Fig. 3(a) and Fig. 3(b), respectively. In free-space, the isolation is better than 17 dB between all antenna ports and the −10 dB impedance bandwidth is 18.5 MHz; for the case with the phantom the respective values are 16.7 dB and 23.5 MHz. The total efficiency is shown in Fig. 4; the efficiency drop at 5 GHz due to the phantom is from 91% to 52%, 49% to 37%, 49% to 36%, 87% to 67% and 87% to 70% for ports 1, 2, 3, 4, and 5, respectively. Note that the bottom patch (excited using port 1) shows the largest efficiency deterioration. This can be explained by its close proximity to the phantom compared to the other patches.

IV. AoA Performance of the Proposed Antenna

Because the proposed wrist-worn antenna offers unidirectional beamsteering in the horizontal plane (xy-plane in Fig. 1), therefore, the Angle of Arrival (AoA) estimation performance is also investigated in the same plane (xy-plane, $\theta = 90°$). The AoA estimation technique used in this work is the MUltiple SIgnal Classification (MUSIC) algorithm [14] implemented using MATLAB, and the performance is evaluated in terms of Mean Absolute Error (MAE) between the MUSIC estimated angle and the actual incident angle.

Fig. 5 shows the AoA performance of the proposed wrist-worn antenna. The results are obtained using 10 dB Signal-to-Noise Ratio (SNR) and 100 snapshots. In free-space the antenna achieves MAE smaller than 0.3°. It can be seen that the MAE increases when the effects of the phantom are included. The performance with the phantom is investigated for different widths (w) of the forearm phantom. A slight increment of the MAE is observed when the width is increased from 60 mm to 80 mm. Nevertheless, in all the investigated cases the MAE stays below 0.45°.

The results shown in Fig. 5 also show MAE peaks in the cases with the phantom (around 40°, 140°, 215°, and 340°). This can be explained by the tilts and asymmetries introduced by the phantom in the radiation pattern of the antenna. This was verified by studying the beamsteering of the antenna around the same angles. For 0° and 180° directions the main beams are exactly at the center of the phantom's width ($y = w/2$) [as shown in Fig. 6(a)]; Hence, the patterns are distorted in a uniform way from both $-y$ and $+y$ directions, leading to low MAE. However, this also results in reduced realized gains (1.29 dBi) around these directions. For 90° and 270° directions low MAE and peak realized gains (4.26 dBi) are observed. This is because the main beams fall in the orthogonal plane ($yz-$plane) in respect to the plane containing the phantom length ($xz-$plane) [see Fig. 6(b)].

Conclusion

In this work we proposed a wrist-worn antenna capable of unidirectional beamsteering across the entire horizontal plane. A human forearm phantom was integrated into the study to investigate the performance of the antenna in the user's wrist. It was demonstrated that when including the phantom the system still offers up to 4.26 dBi of realized gain. These results were used to investigate for the first time in the open-literature the Angle of Arrival Estimation from a wrist-worn antenna, where the estimated errors using the largest diameter of the analyzed phantom are below 0.45°. Future studies will include experimental verifications of the proposed system.

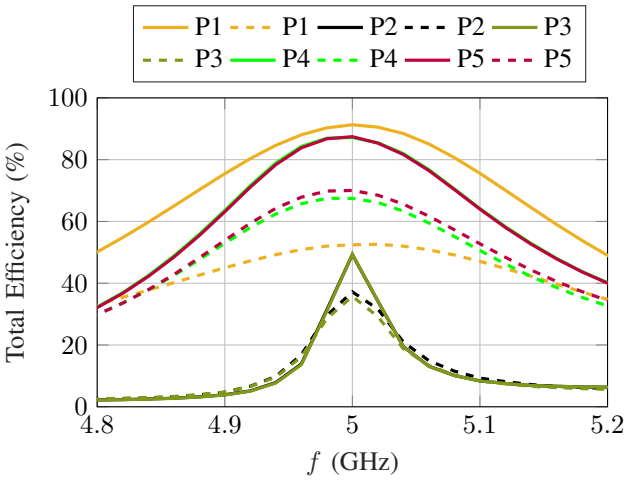

Fig. 4. Simulated total efficiency of the antenna in free-space (solid lines) and with the human forearm phantom (dashed lines).

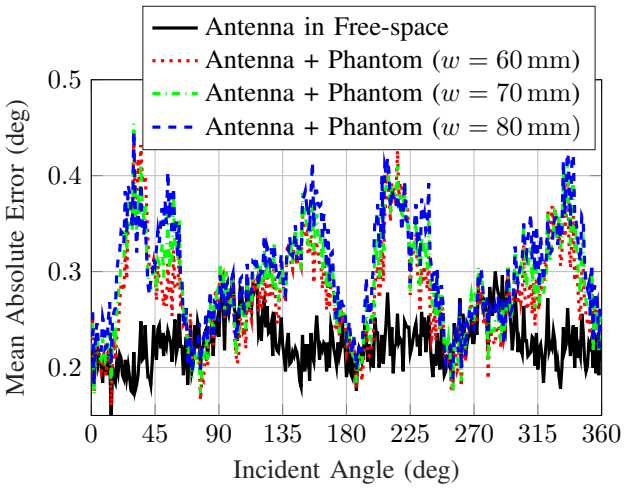

Fig. 5. Comparisons of the Angle of Arrival estimation performance using MUSIC algorithm in 10 dB SNR environment with 100 snapshots.

Acknowledgment

This publication has emanated from research conducted with the financial support of Science Foundation Ireland under Grant number 18/SIRG/5612.

References

[1] J.W. Kim, J. H. Lim, S. M. Moon, and B. Jang, "Collecting health lifelog data from smartwatch users in a privacy-preserving manner", *IEEE Trans. Consum. Electron.*, vol. 65, no. 3, pp. 369–378, Aug. 2019.

[2] S. Lopez-Soriano and J. Parron, "Design of a Small-Size, Low-Profile, and Low-Cost Normal-Mode Helical Antenna for UHF RFID Wristbands", *IEEE Antennas Wirel. Propag. Lett.*, vol. 16, pp. 2074-2077, 2017.

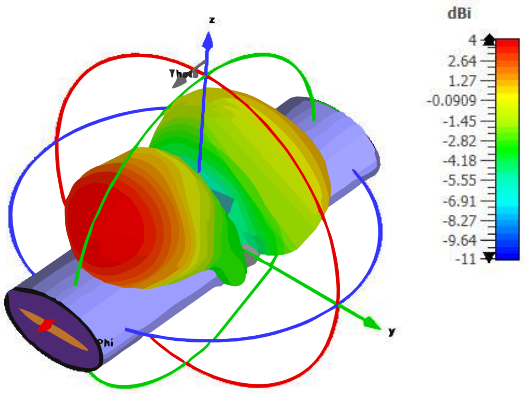

(a)

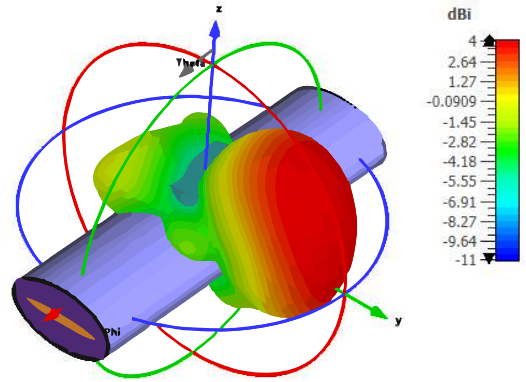

(b)

Fig. 6. 3D visualization of the realized gain for $xy-$plane beamsteering of the proposed system: (a) 0° and (b) 90°. Note that the pattern tilts because of the phantom are symmetrical when the beam is directed towards the center of the phantom as seen in (a), and no pattern tilts are observed when the beams are directed towards the orthogonal $yz-$plane (b).

[3] K. Zhao, Z. Ying and S. He, "Antenna designs of smart watch for cellular communications by using metal belt", *European Conference on Antennas and Propagation (EuCAP)*, 2015, pp. 1-5.

[4] S. Su and Y. Hsieh, "Integrated Metal-Frame Antenna for Smartwatch Wearable Device", *IEEE Trans. Antennas Propag.*, vol. 63, no. 7, pp. 3301-3305, July 2015.

[5] M.-A. Chung and C.-F. Yang, "Built-in antenna design for 2.4 GHz ISM band and GPS operations in a wrist-worn wireless communication device", *IET Microw. Antennas Propag.*, vol. 10, no. 12, pp. 1285–1291,Sep. 2016.

[6] S. Kumar et al., "A Bandwidth-Enhanced Sub-GHz Wristwatch Antenna Using an Optimized Feed Structure", *IEEE Antennas Wireless Propag. Lett.*, vol. 20, no. 8, pp. 1389-1393, Aug. 2021.

[7] D. Wu and S. W. Cheung, "A Cavity-Backed Annular Slot Antenna With High Efficiency for Smartwatches With Metallic Housing", *IEEE Trans. Antennas Propag.*, vol. 65, no. 7, pp. 3756-3761, July 2017.

[8] J. Chen, M. Berg, V. Somero, H. Y. Amin, and A. Pärssinen, "A multiple antenna system design for wearable device using theory of characteristic mode", *Proc. 12th Eur. Conf. Antennas Propag.*, 2018, pp. 1–5.

[9] M.-A. Chung, "Embedded 3D multi-band antenna with ETS process technology covering LTE/WCDMA/ISM band operations in a smart wrist wearable wirelessmobile communication device design", *Microw., Antennas, Propag.*, vol. 14, no. 1, pp. 93–100, 2020.

[10] A. Zandamela, et al., "On the Efficiency of Miniaturized 360° Beam-Scanning Antenna", *2019 13th European Conference on Antennas and Propagation (EuCAP)*, Krakow, Poland, 2019.

[11] A. Zandamela, et al., "Digital pattern synthesis with a compact MIMO antenna of half-wavelength diameter," *AEÜ – Int. J. Electron. Commun.*, vol. 135, Jun. 2021.

[12] C. Gabriel, "Compilation of the dielectric properties of body tissues at RF and microwave frequencies", Report N.AL/OE-TR-, Brooks Air Force Base, Texas (USA), June 1996, http://niremf.ifac.cnr.it/tissprop/.

[13] RJ. Maughan, JS. Watson , and J. Weir, "The relative proportions of fat, muscle and bone in the normal human forearm as determined by computed tomography" *Clin Sci (Lond)*, June 1984.

[14] R. Schmidt, "Multiple emitter location and signal parameter estimation", *IEEE Trans. Antennas Propag.*, vol. 34, no. 3, pp. 276–280, 1986.